Proc. Natl. Acad. Sci. USA
Vol. 77, No. 1, pp. 614–618, January 1980
Microbiology

Molecular cloning of infectious integrated murine leukemia virus DNA from infected mouse cells

(restriction endonucleases/transfection/Southern blotting/DNA heteroduplex mapping)

DOUGLAS R. LOWY*, ELAINE RANDS*, SISIR K. CHATTOPADHYAY†, CLAUDE F. GARON‡, AND GORDON L. HAGER§

*Dermatology Branch, National Cancer Institute, †Pediatric Oncology Branch, National Cancer Institute, ‡Laboratory of Biology of Viruses, National Institute of Allergy and Infectious Diseases, and §Tumor Virus Genetics Branch, National Cancer Institute, National Institutes of Health, Bethesda, Maryland 20205

Communicated by Robert J. Huebner, October 3, 1979

ABSTRACT **The lack of an endonuclease *Eco*RI site in the AKR murine leukemia virus (MuLV) DNA genome was utilized to molecularly clone, in Charon 4A λ DNA, integrated infectious AKR MuLV DNA isolated from productively infected mouse cells. Three λ–mouse recombinants (clones 614, 621, and 623) were selected by virtue of their reactivity with AKR MuLV [^{32}P]cDNA. Clones 614 and 623 contained the complete AKR MuLV DNA flanked by nonviral cell sequences of which no more than 100 base pairs beyond the viral DNA appear to be shared. DNAs from both clones 614 and 623 were highly infectious for mouse cells and yielded N-tropic ecotropic MuLV; the specific infectivity of the DNA and the titer of the derived virus was more than 10-fold higher with 623. Clone 621 contained only some viral DNA and was not infectious under similar conditions.**

Retroviruses replicate via a DNA intermediate, which is incorporated into high molecular weight cell DNA. Several unintegrated infectious linear and circular viral DNAs have been found in acutely infected cells (1–5), but the actual precursor to the integrated viral DNA, which is the form that is found in chronically infected cells, has not yet been established. Integrated retroviral DNA has a preferred orientation (6, 7); the structure of the integrated DNA is similar to that of the unintegrated linear viral DNA. This latter molecule has been shown to contain a direct repetition at each end of the molecule (8, 9). In murine type C viral DNA, this repetition is about 0.65 kilobase pairs (kbp); it includes sequences derived from both the 3′ and 5′ ends of the viral RNA (10–12).

The unique orientation of the integrated viral DNA contrasts with the multiple cellular integration sites at which the viral DNA has been found (6, 7, 13–15). Some, but not all, integrated viral DNAs are infectious (16, 17). It is not known whether this limitation is determined principally by the integrated viral DNA, the cell DNA integration site, or both. The resolution of this problem is complicated because productively infected cells acquire several copies of the viral DNA, and it is difficult to determine whether all, or only some, of these copies are biologically active. It is also not known if the cellular integration sites contain endogenous retroviral sequences, are structurally similar to each other, or are totally different.

We have begun to approach these and related questions by the molecular cloning of integrated type C retroviral DNA. In this communication, we report the molecular cloning in λ phage of three integrated murine leukemia virus DNA molecules from a chronically infected mouse cell line. Each cellular integration site is different, and two of the molecules are infectious.

The publication costs of this article were defrayed in part by page charge payment. This article must therefore be hereby marked "*advertisement*" in accordance with 18 U. S. C. §1734 solely to indicate this fact.

MATERIALS AND METHODS

Virus and Cells. The cells lines were negative for mycoplasma (tested by Flow Laboratories). The AKR ecotropic murine leukemia virus (MuLV) that was used in deriving the restriction endonuclease map for the unintegrated linear viral DNA and for infecting the cell line that was used for the molecular cloning was provided by J. W. Hartley and W. P. Rowe. This virus had been isolated from a young nonleukemic mouse that was congenic for the *Akv-1* locus on a predominantly NIH Swiss genetic background (18). It had been passed four times on mouse SC-1 cells (19) and was then endpoint diluted once and used to infect NIH 3T3 cells at low multiplicity of infection (0.2). Sixteen hours later, the cells were biologically cloned as single cells in microtiter wells. One of the virus-positive clonal lines (11B3) was then used for the isolation of the DNA for molecular cloning. Because it produced more virus than line 11B3, a second clonal line (11D2) was used as the source of virus for the acutely infected cells from which the restriction endonuclease map for unintegrated AKR MuLV was derived. Identical restriction patterns were found for unintegrated viral DNA when line 11B3 was used as the source of virus. Virus titers were determined by the XC plaque test (20) on secondary NFS (an inbred NIH Swiss mouse strain that is sensitive to N-tropic MuLV) and secondary BALB/c cells. For transfections of viral DNA, the NIH 3T3 cell line was used; cells were assayed for XC plaques 1 week after transfection (21).

Molecular Cloning. The EK2-certified λ vector Charon 4A (22) was utilized in P2 containment under conditions prescribed in the revised *NIH Guidelines for Recombinant DNA Research*. After digestion of vector DNA with restriction endonuclease *Eco*RI, vector arms were isolated, mixed with *Eco*RI-digested mouse DNA from fractions 32 and 33 from the preparative gel electrophoresis shown in Fig. 2, ligated with phage T4 ligase, packaged *in vitro* into infectious λ particles, and plated on *Escherichia coli* DP50 *supF* (12–22). By using the AKR MuLV [^{32}P]cDNA probe described in Table 1, phage plaques were assayed *in situ* for λ–AKR MuLV recombinants; these were then subcloned and amplified as described (12).

RESULTS

Before attempting to isolate the integrated AKR ecotropic MuLV DNA, it was necessary to find a suitable restriction endonuclease that would preserve the infectivity of the integrated viral DNA (23) and to derive a preliminary restriction endonuclease map of the viral DNA so that molecularly cloned DNA could be compared with this map. The restriction endonuclease analysis was performed on the three predominant unintegrated

Abbreviations: kbp, kilobase pairs; MuLV, murine leukemia virus.

Table 1. Restriction endonuclease cleavage products of unintegrated linear and circular AKR MuLV DNAs

Enzymes	Sizes of fragments, kbp						
8.8-kbp linear viral DNA							
Xho I	4.5	4.3					
Sma I	4.8	1.7	1.4	0.5	0.4	0.1	
Kpn I	3.9	2.8	1.4	0.5	0.1		
Xho I + *Sma* I	4.1	1.7	1.4	0.6	0.5	0.4	0.1
Xho I + *Kpn* I	2.8	2.8	1.4	1.1	0.5	0.1	
8.8-kbp circular DNA							
Sma I	4.8	1.7	1.4	0.6	0.4		
Kpn I	3.9	2.8	1.4	0.6			
8.2-kbp circular DNA							
Sma I	4.8	1.7	1.4	0.4			
Kpn I	3.9	2.8	1.4				

Unintegrated viral DNA was isolated by the Hirt procedure from NIH 3T3 cells 20 hr after infection (21). Hirt supernatant DNA (10 mg) was then subjected to preparative electrophoresis in a 1% agarose gel (25), and multiple 15-ml fractions were collected. This fractionation separated linear and supercoiled viral DNA by virtue of the latter's faster mobility (12). After restriction endonuclease digestion, the completeness of which was monitored by the addition of wild-type λ DNA, the DNAs were electrophoresed in a 1% agarose gel at 35 V for 16 hr, transferred to nitrocellulose filters (26), and hybridized with an AKR MuLV [^{32}P]cDNA probe that had been synthesized from virion RNA in a reaction catalyzed by avian myeloblastosis virus DNA polymerase and primed with calf thymus DNA oligomers. The 0.1-kbp fragments were not visualized directly. Their presence was inferred from the 0.6 kbp *Sma* I and *Kpn* I fragments seen in the 8.8-kbp circular DNA and by analogy with Moloney MuLV (11).

forms of AKR MuLV DNA found in newly infected cells. These forms, which were analogous to those already described for murine and avian retroviral DNAs (8–12), were an 8.8-kbp linear viral DNA and two covalently closed circular viral DNAs, 8.2 and 8.8 kbp, respectively.

It was first determined that *Eco*RI did not cleave the 8.8-kbp linear DNA or diminish its infectivity, and the infectivity of high molecular weight DNA isolated from NIH 3T3 cells productively infected with AKR MuLV remained intact (data not shown). DNA from uninfected NIH 3T3 cells was not infectious in this assay (23). The restriction endonuclease map of the 8.8-kbp linear DNA was then derived for the enzymes *Xho* I, *Sma* I, and *Kpn* I. The latter two enzymes were chosen because they have been found to cleave Moloney MuLV DNA (10, 11) and Friend MuLV DNA (24) in the repeat sequences. If they cleaved AKR MuLV at the same sites, it would permit the analysis of more than 8 kbp of internal viral fragments in integrated viral DNA. As shown in Fig. 1*A* and summarized in Table 1, *Xho* I digestion cleaved the viral DNA once, generating two fragments of similar size. *Sma* I and *Kpn* I digestion generated six and five fragments, respectively. To order the restriction enzyme sites, the two *Xho* I fragments (4.6 and 4.3 kb) were isolated after electrophoresis (ref. 27; Fig. 1*A*, lanes a and c), and each fragment was then digested with *Sma* I or *Kpn* I. Because sequences derived from the 3′ end of the viral RNA have been shown to be present near both termini of linear retroviral DNA, a [^{32}P]cDNA probe specific for the 3′ sequences of the AKR MuLV RNA was then hybridized with the viral DNA to determine which fragments contained 3′ sequences. This probe hybridized to both *Xho* I fragments, but it hybridized with only two of the *Kpn* I and *Sma* I fragments (Fig. 1*B*). Analysis of these results yielded the preliminary map of the unintegrated linear viral DNA shown in Fig. 4. As expected for enzymes that cleaved the viral DNA in the repeat region, restriction of the 8.2- and 8.8-kbp circular viral DNAs generated all the internal *Sma* I and *Kpn* I cleavage products present in the linear DNA (Table 1).

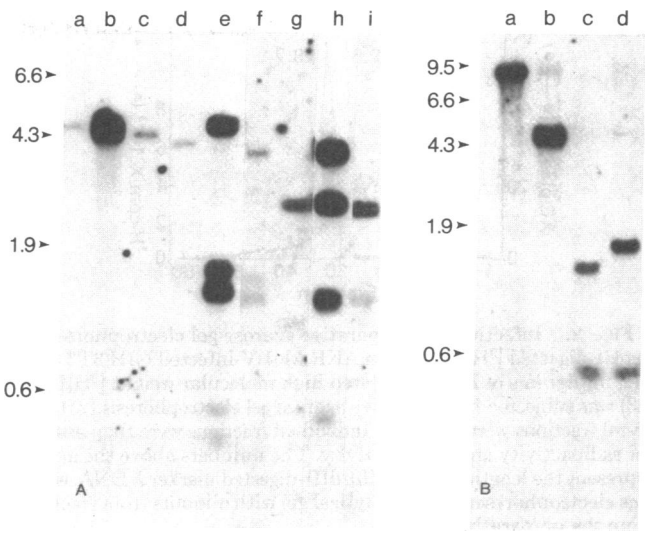

FIG. 1. Southern blot analysis of restriction endonuclease-digested unintegrated linear AKR MuLV DNA. DNAs were transferred to nitrocellulose filters and hybridized as described for Table 1. The numbers represent the length in kbp of *Hin*dIII-digested marker λ DNA. (*A*) Analysis of cleavage products of the 8.8-kbp linear viral DNA and the isolated *Xho* I fragments after hybridization with the representative AKR MuLV [^{32}P]cDNA probe. The 8.8-kbp viral DNA is shown after digestion with *Xho* I (lane b), *Sma* I (lane e), and *Kpn* I (lane h). The isolated 4.5-kbp *Xho* I fragment is shown without further digestion (lane a) and after digestion with *Sma* I (lane d) and *Kpn* I (lane g). The isolated 4.3-kbp *Xho* I fragment is shown without further digestion (lane c) and after digestion with *Sma* I (lane f) and *Kpn* I (lane i). (*B*) Analysis of the cleavage products of the 8.8-kbp linear viral DNA after hybridization with [^{32}P]cDNA specific for the 3′ end of the viral RNA (24). The DNA is shown before digestion (lane a) and after digestion with *Xho* I (lane b), *Kpn* I (lane c), and *Sma* I (lane d).

The linear AKR ecotropic MuLV DNA was oriented with respect to the 3′ and 5′ ends of the viral RNA by comparison with the cleavage products of a *Sma* I digest of the unintegrated linear DNA of AKR MuLV MCF 247, which represents a viral substitution mutant of AKR ecotropic MuLV whose region of nonhomology near the 3′ end of the viral RNA has been previously mapped (28). The *Sma* I fragments of MCF 247 were identical in size to those found with the ecotropic viral DNA, except that the 1.7- and 0.4-kbp fragments of the ecotropic viral DNA were replaced by a poorly hybridizing 2.0-kbp fragment in the MCF 247 DNA (data not shown). This result placed these fragments at the 3′ end of the viral DNAs. With this orientation, four of the five *Sma* I and three of the four *Kpn* I sites in AKR ecotropic MuLV DNA are similar in location to the sites reported for Moloney MuLV DNA (10, 11).

Molecular Cloning of Viral DNA. Viral DNA was cloned from productively infected mouse cells. Although cells of a heterologous species could be infected with a murine ecotropic virus, it would be potentially more informative to characterize the flanking host cell sequences in the homologous species. In particular, it would be possible to determine if the viral DNA is integrated in tandem with crossreacting endogenous viral DNA sequences, which are present in all mice (*Mus musculus*) (18). Some mouse strains contain complete copies of endogenous ecotropic MuLV that might be confused with the AKR MuLV; NIH 3T3 cells were therefore chosen, because the DNA of these cells contains multiple copies of sequences that crossreact with about two thirds of the AKR MuLV but it lacks some of the AKR MuLV genome (18).

Prior to molecular cloning, the cells were biologically cloned

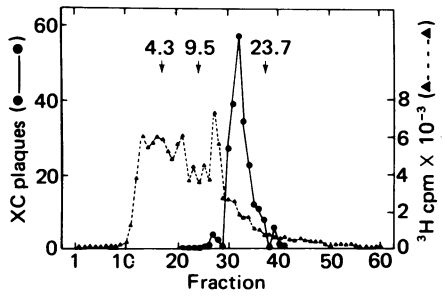

FIG. 2. Infectivity of preparative agarose gel electrophoresis of *Eco*RI-digested [^{3}H]DNA from AKR MuLV-infected NIH 3T3 cells. Ten milligrams of *Eco*RI-digested high molecular weight [^{3}H]DNA (23) was subjected to preparative agarose gel electrophoresis (25), and 15-ml fractions were collected. Individual fractions were than assayed for radioactivity and for infectivity. The numbers above the arrows represent the length in kbp of *Hin*dIII-digested marker λ DNA, which was electrophoresed in an analytical gel with aliquots from fractions from the preparative gel.

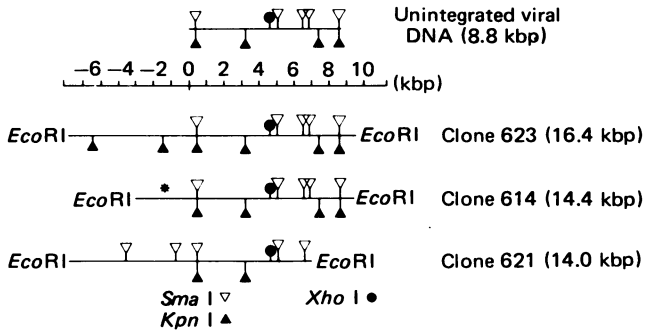

FIG. 4. Structure of unintegrated and integrated AKR MuLV DNA. Structure of the unintegrated viral DNA is given with the sequences corresponding to the 5′ portion of the viral RNA on the left and the sequences corresponding to the 3′ portion of the viral RNA on the right. The structure of clone 614 shown is that of the largest insert of this clone; two smaller forms (13.3 and 12.0 kbp, respectively) have also been detected. Both molecules contain deletions within the *Eco* RI + *Sma* I fragment on the left end of the molecule (marked with an asterisk).

after exogenous infection with AKR MuLV. *Eco*RI-digested DNA was subjected to preparative electrophoresis and the fractions containing DNA of 6–25 kbp were assayed for infectivity. By screening for viral DNA in this manner, the fractions containing infectious DNA could be positively selected. This approach also avoided the potential problem of distinguishing biochemically among the endogenous viral sequences in NIH DNA, the infectious AKR MuLV DNA sequences, and possibly noninfectious AKR MuLV sequences. A peak of infectivity corresponding to 12–18 kbp was found in the fractionated DNA (Fig. 2). DNA from the most infectious fractions was ligated to the *Eco*RI arms of Charon 4A λ DNA, packaged into infectious λ phage particles, and amplified in an EK2 *E. coli* host. Of the approximately 5×10^4 plaques generated, three reacted strongly with AKR MuLV [^{32}P]cDNA and were propagated for analysis of their DNA.

Analysis of λ–Mouse Recombinant DNA. Fig. 3 shows the agarose gel electrophoresis pattern of the three λ–mouse recombinant DNA preparations after digestion with *Eco*RI, *Sma* I, and *Kpn* I. In the ethidium bromide-stained gel, the *Eco*RI digests reveal, in addition to the Charon 4A arms (19.8 kbp and 10.9 kbp), a 16.4-kbp band in clone 623, three bands between 12 and 15 kbp in clone 614, and a 14.4-kbp band in clone 621. In the autoradiogram, which represents the Southern blot analysis of the DNA from the gel after its transfer to a nitrocellulose filter and hybridization with AKR MuLV [^{32}P]cDNA, the *Eco*RI cleavage products reveal hybridization to each of the non-λ DNA bands. Clones 623 and 614 contained all the internal *Kpn* I and *Sma* I fragments of unintegrated linear AKR MuLV DNA, whereas in clone 621 some internal *Sma* I and *Kpn* I fragments were absent. The *Eco*RI + *Sma* I and *Eco* RI + *Kpn* I double digests suggest the fragment orientation shown in Fig. 4. The validity of this map has been confirmed through the use of isolated restriction fragments. The results are consistent with the complete AKR MuLV DNA being present in clone 623 and 614, whereas clone 621 is missing a portion of the viral DNA. In each instance, the restriction fragment that should contain the 0.5-kbp *Sma* I or *Kpn* I fragments hybridizes with the [^{32}P]viral cDNA. However, the restriction fragments to the left of this fragment do not hybridize to the cDNA. These results suggest that most or all of the direct terminal repeat present in the unintegrated linear DNA is retained in the integrated linear molecule. Similar results have been noted pre-

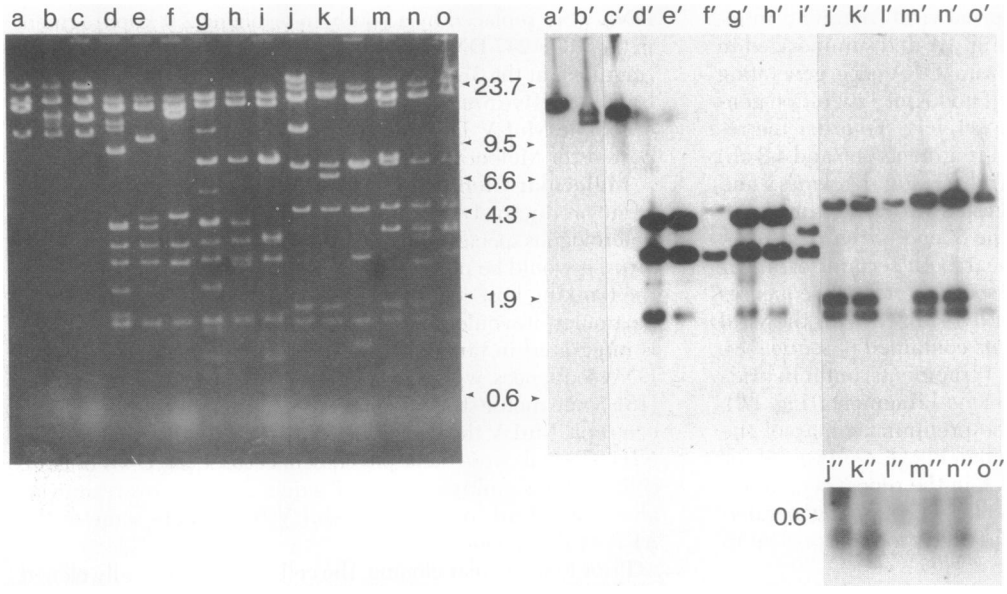

FIG. 3. Agarose gel electrophoresis of λ–mouse recombinant DNAs from clones 623, 614, and 621. *Eco*RI, lanes a, b, c; *Kpn* I, lanes d, e, f; *Eco* RI + *Kpn* I, lanes g, h, i; *Sma* I, lanes j, k, l; *Eco*RI + *Sma* I, lanes m, n, o. Clone 623, lanes a, d, g, j, n; clone 614, lanes b, e, h, k, n; clone 621, lanes c, f, i, l, o. One microgram of DNA was electrophoresed in each lane, transferred to a nitrocellulose filter, and hybridized with AKR MuLV [^{32}P]cDNA. (*Left*) UV-fluorescence photograph of the ethidium bromide-stained gel; (*Right*) autoradiograph of the filter hybridization. a′–o′ on the right correspond to lanes a–o on the left. Lanes j″–o″ represent an overexposure of the lower portion of lanes j′–o′. The numbers represent the location of *Hin*dIII marker wild-type λ DNA fragments.

viously for integrated avian retroviral DNA (6, 7). These results also suggest that the flanking cell sequences are different in each clone and do not contain viral DNA.

The heterogeneity noted in the DNA of clone 614 was characterized by an analysis of subclones of this λ–mouse recombinant. Three different insert DNA molecules have been found: they are 14.4, 13.6, and 12.0 kbp, respectively. They differ only in the length of the leftward-most *Sma* I (or *Kpn* I) fragment (see Fig. 4) and appear to represent spontaneous deletions of flanking nonviral mouse DNA, because this fragment continues to show hybridization to the AKR MuLV [^{32}P]cDNA (data not shown).

The extent of sequence homology between clones 614 and 623 was also compared by heteroduplex analysis. The structure formed with the two *Eco*RI inserts contained a single large duplex region in the middle of each molecule with single-stranded forks at each end (Fig. 5*A*). This region of homology was identical to the contour length of molecularly cloned 8.8-kbp Friend MuLV DNA derived from supercoiled viral DNA, which contains two copies in tandem of the 0.65-kbp repeat sequences (24). To verify that the region of homology between clones 614 and 623 was confined to the viral DNA, a heteroduplex of the Friend MuLV DNA with clone 623 was formed. Under the conditions used here, the entire Friend MuLV DNA formed a duplex molecule with clone 623 (Fig. 5*B*), although numerous differences between the two viruses have been found in the restrictions endonuclease map of the two viral DNAs (24) and in liquid hybridization carried out under stringent conditions (30). The length of the duplex formed between the Friend MuLV DNA and clone 623 was also identical to that found between clone 623 and 614 (Fig. 5). These results indicated that the detectable homology between clones 614 and 623 was limited to the viral DNA sequences, that no detectable viral sequences were present in the flanking cell sequences, and that a virtually complete copy of the 0.65-kbp sequences was present at each end of the viral DNA.

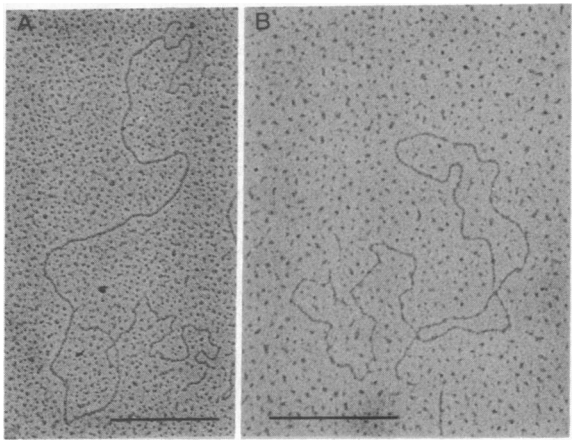

C

DNA molecules hybridized	Contour length of duplex DNA, μm
Clone 623 and clone 614	3.029 ± 0.077 (25)
Clone 623 and Friend MuLV (8.8 kbp)	2.952 ± 0.068 (21)
Friend MuLV (8.8 kbp)	3.040 ± 0.093 (41)

FIG. 5. Heteroduplex analysis of clones 614 and 623. *Eco*RI-digested DNA was reannealed in 50% (vol/vol) formamide/0.1 M Tris·HCl, pH 8.5/1 mM EDTA for 2 hr at 37°C. DNA was mounted for microscopy by the formamide procedure (29). (*A*) Hybrid molecule formed between the *Eco*RI inserts of the DNA from clones 614 and 623. A linear duplex region is seen with forks at each end. (*B*) Hybrid molecule formed between the *Eco*RI insert of clone 623 and the 8.8-kbp Friend MuLV DNA cloned from supercoiled viral DNA (clone 77 in ref. 24). The Friend MuLV DNA was cloned at its unique *Eco*RI site. It contains tandem copies of the 0.65-kbp repeat sequences and is permuted with respect to the linear viral DNA (24). The hybrid formed shows the expected circular duplex region with two single-stranded tails, which presumably represent the cell sequences of clone 623. The bars in *A* and *B* represent 0.5 μm. (*C*) Contour lengths (±SEM) of the duplex regions of the DNA hybrid structures and of the Friend MuLV DNA. The numbers in parenthesis indicate the number of molecules analyzed.

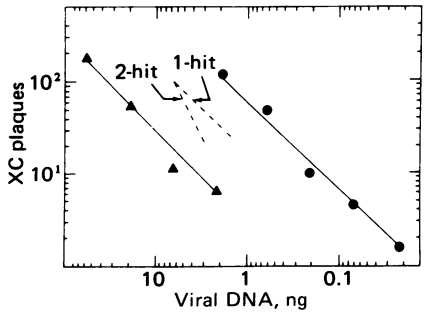

FIG. 6. Infectivity of DNA from clones 623 (●) and 614 (▲). The amount of viral DNA applied to the dishes was calculated by using 8.8 kbp of the DNA to represent the AKR MuLV DNA. The broken lines represent theoretical one-hit and two-hit titration curves.

Infectivity of Cloned DNA. Although the restriction endonuclease digestion analysis of clones 614 and 623 suggested that both contained the complete viral genome, it remained to be determined if these molecules were biologically active. When assayed on NIH 3T3 cells, DNAs from both clones were highly infectious. Their infectivity fell with single-hit kinetics (Fig. 6), which implies that each XC plaque was derived from a single DNA molecule. In the same assay clone 621, which had been shown to lack some AKR MuLV DNA sequences, was not infectious. It should be noted that the specific infectivity of clone 623 was more than 10-fold greater than that of clone 614. In the experiment shown in Fig. 6, the DNA from clone 614 was primarily that of the larger insert. The possibility that differences in specific infectivity might arise with different subclones of 614 was therefore tested. As shown in Table 2, however, the specific infectivities of subclones of 614 were virtually identical regardless of the size of the DNA insert. The infectivities of the recombinant DNA samples were equally efficient whether or not the DNA was digested with *Eco*RI, and the infectivity of clone 623 was not significantly altered by the addition of equal amounts of clone 621 or clone 614. However, infectivity was abolished after digestion with *Kpn* I or *Sma* I (data not shown).

The viruses isolated after transfection with clone 614 and 623 were both N-tropic, ecotropic, XC plaque-forming viruses, as is true of AKR MuLV. However, the titer of MuLV in supernatant fluids from cells chronically infected with virus derived from clone 623 was more than one order of magnitude greater than the titer of virus derived from clone 614 (790,000 vs. 63,000 plaque-forming units/ml).

Table 2. Infectivity of integrated AKR murine leukemia virus DNA

DNA clone	Insert length, kbp	Infectivity, plaque-forming units/μg viral DNA
623	16.4	200,000
614-12	14.4	8,200
614-4	13.3	11,000
614-11	12.0	12,000
621	12.0	<2

DISCUSSION

In the experiments reported here, three different λ–mouse recombinant DNAs have been isolated from a mouse cell line chronically infected with AKR MuLV. The flanking cell sequences for each molecule were different, indicating that the integration sites were different. Clones 614 and 623 contained the complete AKR MuLV DNA and were highly infectious, whereas in the same assay clone 621, which lacked some viral DNA sequences, was not infectious. It is not yet clear whether clone 621 represents a form of the exogenously infecting AKR MuLV with a deletion or whether it represents endogenous sequences that crossreact with the AKR MuLV cDNA. The two infectious viral DNA genomes reported here reveal several structural and biologic features not previously documented for retroviral DNA. Previous reports indicated that type C viral DNA can integrate in multiple sites, but the biologic activity of DNA from a specific integration site had not been evaluated in the murine system. The infectivity results show directly that infectious viral DNA may be integrated at more than one site. As recently suggested for avian viruses (31), the murine viral DNAs were not integrated in tandem with the ecotropic virus-related endogenous DNA sequences present in NIH cells.

Previous reports of integrated retroviral DNA have indicated that most or all of the direct repeat sequences present at the termini of the unintegrated viral DNA are also present in the integrated viral DNA. The results reported here are consistent with a similar structure for integrated MuLV DNA (6, 7, 32). In the present report, we have also made a preliminary determination of the potential degree of homology between different integration sites. By heteroduplex analysis, the only detectable homology between clones 614 and 623 was contained within the viral sequences. Given the limitations inherent in the heteroduplex method, the results suggest that the integration sites of clones 614 and 623 share no more than 0.1 kbp of homology, unless part of the viral DNA was in the integration sites prior to infection. Further studies are needed to more carefully define the homology between the two different clones and their integration sites.

An unanticipated finding of this report is the difference of specific infectivity of clones 614 and 623. Virus derived from transfection of clone 614, whose DNA was less infectious than that of clone 623, also had a lower titer in chronically infected cells. This result suggests, but does not prove, that the differences in specific infectivity are due to the viral DNA sequences, rather than to the flanking cellular sequences. If the differences in infectivity are reflected in the viral sequences of the two clones, the heteroduplex mapping results suggest that these differences will be minor, because no deletion or substitution loops were observed. Further studies of the cloned AKR MuLV DNAs should provide insight into the structural basis of the biologic differences between clones 623 and 621. The infectious viral DNAs will also be useful in structural and biologic comparison with the DNAs of endogenous viral genomes.

We thank Drs. Janet W. Hartley, Wallace P. Rowe, and Edward M. Scolnick for encouragement and advice, Ralph Shober for excellent technical assistance, and Lorraine Shaughnessy for typing the manuscript. This work was supported in part by a contract from the National Cancer Institute to Meloy Laboratories, Springfield, VA.

1. Smotkin, D., Gianni, A. M., Rozenblatt, S. & Weinberg, R. A. (1975) *Proc. Natl. Acad. Sci. USA* **72,** 4910–4913.
2. Smotkin, D., Yoshimura, F. K. & Weinberg, R. A. (1976) *J. Virol.* **20,** 621–626.
3. Guntaka, R. V., Richards, O. C., Shank, P. R., Kung, H.-J., Davidson, N., Fritsch, E., Bishop, J. M. & Varmus, H. E. (1976) *J. Mol. Biol.* **106,** 337–357.
4. Fritsch, E. & Temin, H. M. (1977) *J. Virol.* **21,** 119–130.
5. Varmus, H. E., Heasly, S., Kung, H.-J., Opperman, H., Smith, V. C., Bishop, J. M. & Shank, P. R. (1978) *J. Mol. Biol.* **120,** 55–82.
6. Hughes, S. H., Shank, P. R., Spector, D. H., Kung, H.-J., Bishop, J. M., Varmus, H. E., Vogt, P. K. & Breitman, M. L. (1978) *Cell* **15,** 1397–1410.
7. Sabran, J. L., Hsu, T. W., Yeater, C., Kaji, A., Mason, W. S. & Taylor, J. M. (1979) *J. Virol.* **29,** 170–178.
8. Hsu, T. W., Sabran, J. L., Mark, G. E., Guntaka, R. V. & Taylor, J. M. (1978) *J. Virol.* **28,** 810–818.
9. Shank, P. R., Hughes, S. H., Kung, H.-J., Majors, J. E., Quintrell, N., Guntaka, R. V., Bishop, J. M. & Varmus, H. E. (1978) *Cell* **15,** 1383–1395.
10. Yoshimura, F. & Weinberg, R. A. (1979) *Cell* **16,** 323–332.
11. Gilboa, E., Goff, S., Shields, A., Yoshimura, F., Mitra, S. & Baltimore, D. (1979) *Cell* **16,** 863–874.
12. Hager, G. L., Chang, E. H., Chan, H. W., Garon, C. F., Israel, M. A., Martin, M. A., Scolnick, E. M. & Lowy, D. R. (1979) *J. Virol.* **31,** 795–809.
13. Chattopadhyay, S. K., Rowe, W. P. & Levine, A. S. (1976) *Proc. Natl. Acad. Sci. USA* **73,** 4095–4099.
14. Steffen, D. & Weinberg, R. A. (1978) *Cell* **15,** 1003–1010.
15. Bacheler, L. T. & Fan, H. (1979) *J. Virol.* **30,** 657–667.
16. Battula, N. & Temin, H. M. (1977) *Proc. Natl. Acad. Sci. USA* **74,** 281–285.
17. Keshet, E. & Temin, H. M. (1978) *Proc. Natl. Acad. Sci. USA* **75,** 3372–3376.
18. Chattopadhyay, S. K., Rowe, W. P., Teich, N. M. & Lowy, D. R. (1975) *Proc. Natl. Acad. Sci. USA* **72,** 906–910.
19. Hartley, J. W. & Rowe, W. P. (1975) *Virology* **65,** 128–134.
20. Rowe, W. P., Pugh, W. E. & Hartley, J. W. (1970) *Virology* **42,** 1136–1139.
21. Lowy, D. R., Rands, E. & Scolnick, E. M. (1978) *J. Virol.* **26,** 291–298.
22. Blattner, F. R., Blechl, A. E., Denniston-Thompson, K., Faber, H. E., Richards, J. E., Slightom, J. L., Tucker, P. W. & Smithies, O. (1979) *Science* **202,** 1279–1284.
23. Lowy, D. R. (1978) *Proc. Natl. Acad. Sci. USA* **75,** 5539–5543.
24. Oliff, A., Hager, G. L., Chang, E. H., Scolnick, E. M., Chan, H. W. & Lowy, D. R. (1980) *J. Virol.* **33,** 475–486.
25. Polsky, F., Edgell, M. H., Seidman, J. G. & Leder, P. (1978) *Anal. Biochem.* **87,** 397–410.
26. Southern, E. M. (1975) *J. Mol. Biol.* **38,** 503–517.
27. Vogelstein, B. & Gillespie, D. (1979) *Proc. Natl. Acad. Sci. USA* **76,** 615–619.
28. Chien, Y. H., Verma, I. M., Shih, T. Y., Scolnick, E. M. & Davidson, N. (1978) *J. Virol.* **28,** 352–360.
29. Davis, R. W., Simon, M. & Davidson, N. (1971) *Methods Enzymol.* **21,** 413–428.
30. Troxler, D. H., Yuan, E., Linemeyer, D., Ruscetti, S. & Scolnick, E. M. (1978) *J. Exp. Med.* **146,** 639–653.
31. Akiyama, Y. & Vogt, P. H. (1979) *Proc. Natl. Acad. Sci. USA* **76,** 2465–2469.
32. VandeWoude, G. F., Oskarsson, M., Enquist, L. W., Nomura, S., Sullivan, M. & Fischinger, P. J. (1979) *Proc. Natl. Acad. Sci. USA* **76,** 4464–4468.